THE JOURNAL OF BIOLOGICAL CHEMISTRY VOL. 287, NO. 26, pp. 21856–21865, June 22, 2012


# Phosphatidylinositol 4-Kinase IIα Is Palmitoylated by Golgi-localized Palmitoyltransferases in Cholesterol-dependent Manner*[S]

Received for publication, January 31, 2012, and in revised form, April 23, 2012 Published, JBC Papers in Press, April 25, 2012, DOI 10.1074/jbc.M112.348094

**Dongmei Lu[‡], Hui-qiao Sun[‡], Hanzhi Wang[‡], Barbara Barylko[§], Yuko Fukata[¶], Masaki Fukata[¶], Joseph P. Albanesi[§], and Helen L. Yin[‡1]**

*From the Departments of [‡]Physiology and [§]Pharmacology, University of Texas Southwestern Medical Center, Dallas, Texas 75390 and the [¶]Division of Membrane Physiology, Department of Cell Physiology, National Institute for Physiological Sciences, Aichi 444-8787, Japan*

**Background:** Palmitoylation of phosphatidylinositol 4-kinase IIα (PI4KIIα) regulates its function and Golgi localization, and cholesterol depletion delocalizes Golgi PI4KIIα and inhibits activity.
**Results:** Palmitoyl acyltransferases (PATs) that palmitoylate PI4KIIα were identified. Cholesterol extraction inhibited PI4KIIα association with PATs, decreased palmitoylation, and reduced Golgi phosphatidylinositol 4-phosphate.
**Conclusion:** Cholesterol has a critical role in regulating PI4KIIα interaction with PATs and palmitoylation.
**Significance:** This study uncovered a novel mechanism for preferential recruitment of PI4KIIα to Golgi.

**Phosphatidylinositol 4-kinase IIα (PI4KIIα) is predominantly Golgi-localized, and it generates >50% of the phosphatidylinositol 4-phosphate in the Golgi. The lipid kinase activity, Golgi localization, and "integral" membrane binding of PI4KIIα and its association with low buoyant density "raft" domains are critically dependent on palmitoylation of its cysteine-rich $^{173}$CCPCC$^{177}$ motif and are also highly cholesterol-dependent. Here, we identified the palmitoyl acyltransferases (Asp-His-His-Cys (DHHC) PATs) that palmitoylate PI4KIIα and show for the first time that palmitoylation is cholesterol-dependent. DHHC3 and DHHC7 PATs, which robustly palmitoylated PI4KIIα and were colocalized with PI4KIIα in the *trans*-Golgi network (TGN), were characterized in detail. Overexpression of DHHC3 or DHHC7 increased PI4KIIα palmitoylation by >3-fold, whereas overexpression of the dominant-negative PATs or PAT silencing by RNA interference decreased PI4KIIα palmitoylation, "integral" membrane association, and Golgi localization. Wild-type and dominant-negative DHHC3 and DHHC7 co-immunoprecipitated with PI4KIIα, whereas non-candidate DHHC18 and DHHC23 did not. The PI4KIIα $^{173}$CCPCC$^{177}$ palmitoylation motif is required for interaction because the palmitoylation-defective SSPSS mutant did not co-immunoprecipitate with DHHC3. Cholesterol depletion and repletion with methyl-β-cyclodextrin reversibly altered PI4KIIα association with these DHHCs as well as PI4KIIα localization at the TGN and "integral" membrane association. Significantly, the Golgi phosphatidylinositol 4-phosphate level was altered in parallel with changes in PI4KIIα behavior. Our study uncovered a novel mechanism for the preferential recruitment and activation of PI4KIIα to the TGN by interaction with Golgi- and raft-localized DHHCs in a cholesterol-dependent manner.**

Phosphatidylinositol 4-kinases (PI4Ks)[2] generate phosphatidylinositol 4-phosphate (PI4P), which is an essential regulator of membrane trafficking at the Golgi hub and the gatekeeper for entry into the canonical phosphoinositide biosynthetic pathways at the plasma membrane hub (1–3). Mammals have two major classes of PI4Ks, termed type II and type III, and each has two members (PI4KIIα and PI4KIIβ; PI4KIIIα and PI4KIIIβ) (4). Cumulative evidence indicates that these PI4Ks are located in different subcellular compartments and have unique roles. PI4KIIα and PI4KIIIβ are the two major Golgi PI4Ks. PI4KIIα, which generates >50% of the PI4P in the Golgi, resides primarily in the *trans*-Golgi network (TGN) and in endosomes (5–10). PI4KIIα depletion by RNAi blocks the recruitment of the AP-1 and GGA clathrin adaptor proteins to the TGN (5, 11) and inhibits constitutive secretion (5), phagocytosis (12), and the generation and/or trafficking of endosomes (10, 13).

PI4KIIα is unique among the PI4Ks because it behaves predominantly as an integral membrane protein, defined operationally as requiring detergent for solubilization, despite the lack of a *bona fide* transmembrane domain (14, 15). The tight membrane association (henceforth referred to as "integral" with quotation marks to indicate quasi-integral association), enrichment in "raft" microdomains, and predominant localization in the TGN of PI4KIIα are all dependent on *S*-palmitoylation (14). PI4KIIα is palmitoylated in a Cys-rich motif ($^{173}$CCPCC$^{177}$) that is embedded in the catalytic core, and palmitoylation activates PI4KIIα catalytic activity (14). Despite the importance of PI4KIIα palmitoylation for the full spectrum

* This work was supported, in whole or in part, by National Institutes of Health Grants R01 GM66110 and P50 GM21681 (to H. L. Y.) and GM75401 (to J. P. A.).
[S] This article contains supplemental Fig. 1.
[1] To whom correspondence should be addressed: Dept. of Physiology, University of Texas Southwestern Medical Center, 5323 Harry Hines Blvd., Dallas, TX 75390-9040. Tel.: 214-645-6035; Fax: 214-645-6049; E-mail: helen.yin@utsouthwestern.edu.

[2] The abbreviations used are: PI4K, phosphatidylinositol 4-kinase; PI4P, phosphatidylinositol 4-phosphate; TGN, *trans*-Golgi network; PAT, palmitoyl acyltransferase; MβCD, methyl-β-cyclodextrin; EGFP, enhanced green fluorescent protein; DN, dominant-negative.

of PI4KIIα functions (14), the palmitoyl acyltransferases (PATs) that palmitoylate PI4KIIα have not been identified. Furthermore, although recent studies by others have shown that the enzymatic activity and Golgi localization of PI4KIIα and its lateral diffusion within membranes are decreased by cholesterol depletion (9, 16), the relation between cholesterol and PI4KIIα palmitoylation has not been examined.

Humans and mice have 23 phylogenetically conserved PATs that contain a signature Asp-His-His-Cys (DHHC) motif (17–23). Here, we report that PI4KIIα is palmitoylated by at least six DHHC PATs and establish that the primarily Golgi-localized DHHC3 and DHHC7 are *bona fide* PI4KIIα PATs: they colocalized with PI4KIIα in the TGN; their silencing by RNAi decreased PI4KIIα palmitoylation, integral membrane association, and Golgi localization; and they associated with PI4KIIα in pulldown assays. We also show that PI4KIIα palmitoylation is cholesterol-dependent: cholesterol depletion reduced the association of PI4KIIα with DHHCs and decreased its palmitoylation, integral membrane association, and Golgi localization. It also reduced the amount of PI4P at the TGN. Significantly, cholesterol depletion did not decrease DHHC Golgi localization, suggesting that PI4KIIα, and not the DHHCs, is the primary cholesterol-dependent target.

## EXPERIMENTAL PROCEDURES

*Materials*—All reagents were from Sigma-Aldrich unless indicated otherwise. Triton X-100 and reagents for electrophoresis and immunoblotting were from Bio-Rad. Recombinant protein G-Sepharose 4B was from Invitrogen. The antibodies used and their sources are as follows: monoclonal anti-Myc 9E10, polyclonal goat anti-DHHC7 (anti-ZDHHC7 (G-12)), and anti-DHHC3 (anti-GODZ (C-13)) (Santa Cruz Biotechnology, Inc., Santa Cruz, CA); anti-HA (Covance, Princeton, NJ); anti-PI4P (Echelon Bioscience, Salt Lake City, UT); sheep anti-TGN46 (Serotec, Raleigh, NC); anti-GM130 (BD Biosciences); and fluorescently conjugated secondary antibodies (Jackson ImmunoResearch Laboratories, Inc., West Grove, PA).

*Cell Transfection*—HeLa, COS-7, and HEK293 cells were used in different experiments. In general, HeLa cells, which express transfected proteins at relatively low levels, were used for immunofluorescence and RNAi studies. COS-7 cells, which express transfected proteins at moderate levels, were used for co-immunoprecipitation studies. HEK293 cells, which express transfected proteins at high levels, were used in palmitoylation screens. Cells cultured in DMEM containing 10% FBS and antibiotics were transfected with epitope-tagged rat PI4KIIα (15) and mouse DHHC (19) cDNAs using Lipofectamine 2000 (Invitrogen) according to the manufacturer's instructions. Cells were assayed after 12–24 h. siRNAs that target different regions of human DHHC3 or DHHC7 were obtained from Santa Cruz Biotechnology, Inc., and Sigma (DHHC3 siRNA, Santa Cruz sc-75158/Sigma SASI_Hs01_00133396; DHHC7 siRNA, Santa Cruz sc-93249/Sigma SASI_Hs01_00033548). siRNAs were transfected into HeLa cells with RNAiMAX (Invitrogen) and used after 48–68 h.

*[$^3$H]Palmitate Labeling*—Cells transfected with Myc-PI4KIIα with or without HA-DHHC were preincubated for 30 min in DMEM with fatty acid-free BSA (5 mg/ml). They were then labeled with 0.5 mCi/ml [$^3$H]palmitic acid (PerkinElmer Life Sciences) for 4 h in DMEM with fatty acid-free BSA (5 mg/ml) and washed with PBS. In some cases (*e.g.* Fig. 1*B*), cells were scraped with SDS-PAGE sample buffer (62.5 mM Tris-HCl (pH 6.8), 10% glycerol, 2% SDS, 10 mM DTT, and 0.001% bromphenol blue) and boiled for 2 min (18). Proteins were resolved by SDS-PAGE. Gels were treated with Amplify (GE Healthcare) for 30 min, dried under vacuum, and exposed to Kodak Biomax MS at −80 °C. Parallel gels were subjected to Western blotting. Band intensity was analyzed with ImageQuant 5.2 software. In other experiments, Myc-PI4KIIα was immunoprecipitated prior to Western blotting or fluorography (see below) (14).

*Immunoprecipitation*—Cells were homogenized in solution containing 1% Brij 98, 150 mM NaCl, 5 mM $MgCl_2$, 25 mM MES (pH 6.5), 10 mM $Na_4P_2O_3$, 2 mM NaF, 0.1 mM $Na_2VO_4$, and protease inhibitors (14, 24). Lysates were centrifuged at 15,000 × *g* for 15 min at 4 °C, and the resulting supernatants were incubated with recombinant protein G-Sepharose B for 30 min to remove nonspecifically bound proteins. The precleared supernatants were incubated with anti-Myc or anti-HA antibody overnight at 4 °C and subsequently with protein G-Sepharose for 1 h at 4 °C. Beads were collected by centrifugation and washed extensively. Immunoprecipitated proteins were resolved by SDS-PAGE and subjected to Western blotting or fluorography.

*Protein and Palmitate Turnover Measurements*—Cells transfected with Myc-PI4KIIα were incubated with methionine/cysteine-free DMEM for 1 h, labeled with 50 μCi/ml [$^{35}$S]Met/Cys for 1 h, and subsequently chased with unlabeled 2 mM Met/Cys for 2, 4, and 6 h. In parallel, another aliquot of cells was incubated for 1 h in DMEM with 5% dialyzed FBS, labeled with [$^3$H]palmitate for 4 h, and then chased with unlabeled 100 μM palmitate (25). Cells were lysed and immunoprecipitated with anti-Myc antibody. Immunoprecipitated proteins were resolved by SDS-PAGE and analyzed by fluorography.

*Immunofluorescence Microscopy*—To label proteins in cells, in most cases, cells were fixed with 3.7% formaldehyde in PBS for 10 min at room temperature, permeabilized with 0.1% Triton X-100 in PBS for 5 min on ice, blocked with 1% BSA and 3% donkey serum in PBS, and stained with primary antibodies and rhodamine- or FITC-conjugated secondary antibodies. Cells used for GM130 labeling were fixed and permeabilized in methanol at −20 °C for 10 min. Cells were examined using a Zeiss LSM 510 laser scanning confocal microscope.

To label Golgi PI4P, a fixation/permeabilization protocol that was optimized for detecting Golgi PI4P was used (26). All steps were performed at room temperature. Cells on coverslips were fixed with 2% formaldehyde in PBS. After 15 min, coverslips were rinsed in PBS containing 50 mM $NH_4Cl$, and cells were permeabilized by incubation with 20 μM digitonin in buffer A (20 mM PIPES (pH 6.8), 17 mM NaCl, and 2.7 mM KCl) for 5 min. After washing, permeabilized cells were incubated for 45 min with buffer A supplemented with 5% (v/v) donkey serum and 50 mM $NH_4Cl$. Cells were stained with anti-PI4P antibody and rhodamine-conjugated secondary antibody in buffer A with 5% donkey serum. Golgi PI4P intensity was analyzed using ImageJ software.

To assess colocalization, cells coexpressing different tagged proteins were analyzed. For each cell, 10–12 images at a slice interval of 0.3 μm were captured using the Z-stack scanning function of the Zeiss LSM 510 confocal microscope. Colocalization was analyzed using the Zeiss LSM 510 ZEN software. Fluorescent signals within the same voxel were considered to be colocalized and are expressed as percentage colocalization. Ten randomly chosen cells from each group were analyzed in each experiment.

*Preparation of Cytosol and Sequentially Extracted Membrane Fractions*—A sequential extraction procedure described previously was used (14). All solutions were maintained at 4 °C and contained protease and phosphatase inhibitors (50 mM NaF, 50 mM glycerophosphate, 1 mM $Na_2VO_4$, and 10 μM microcystin). Cells expressing Myc-PI4KIIα were washed with ice-cold PBS and scraped from Petri dishes in a solution containing 0.25 M sucrose, 20 mM Tris-HCl (pH 7.5), 0.1 M NaCl, and 1 mM EDTA. Cells were subjected to two freeze-thaw cycles and passed through a 27-gauge needle. Lysates were centrifuged at 1000 × *g* for 5 min to remove unbroken cells and nuclei. The post-nuclear supernatant was then centrifuged at 200,000 × *g* for 15 min to separate the cytosol from the membranes. The resulting membrane pellets were homogenized in solution containing 20 mM Tris-HCl (pH 7.5), 1 M NaCl, and 1 mM EDTA to extract weakly bound peripheral membrane proteins (fraction 1, salt extraction). Membranes were collected by another round of centrifugation (200,000 × *g* for 15 min) and homogenized in 0.1 M sodium carbonate (pH 11) to extract tightly bound peripheral membrane proteins (fraction 2, carbonate extraction). Finally, integrally associated membrane proteins were extracted by homogenization in 1% Triton X-100 (fraction 3, detergent extraction).

*Preparation of Low Buoyant Density Membrane Fractions*—Low buoyant density detergent-resistant membrane raft fractions were prepared using Brij 98 (14, 24). Cells were homogenized in solution containing 1% Brij 98, 150 mM NaCl, 5 mM $MgCl_2$, 25 mM MES (pH 6.5), 10 mM $Na_4P_2O_3$, 2 mM NaF, 0.1 mM $Na_2VO_4$, and protease inhibitors. The lysate (1.5 ml) was mixed with an equal volume of 80% (w/v) sucrose and overlaid with 5.5 ml of 35% sucrose and 3.5 ml of 5% sucrose in buffer without Brij 98. Following centrifugation at 210,000 × *g* for 16 h at 4 °C in an SW40 rotor, 1-ml fractions were collected from the bottom of the tube, and equal aliquots were subjected to SDS-PAGE and immunoblotting.

*Cholesterol Depletion and Repletion*—Cells were sterol-depleted by incubation with 10 mM methyl-β-cyclodextrin (MβCD; Sigma C4555) for 30 min at 37 °C in serum-free DMEM (9). Cholesterol repletion was performed by incubating cells with DMEM with 5% lipoprotein-deficient serum with or without 2.5 mM water-soluble cholesterol (complexed with MβCD; Sigma C4951) for 2 h.

*Statistical Analysis*—Quantitative results are expressed as means ± S.E. Comparison between groups was performed using one-way analysis of variance.

## RESULTS

*PI4KIIα Protein and Palmitate Turnover*—Palmitoylation is a potentially reversible post-translational modification (27–30). We compared the rates of Myc-PI4KIIα turnover at the protein and palmitate levels by pulse-chase labeling. [$^{35}$S]Met/Cys turned over with a half-life of 4.5 h, whereas [$^3$H]palmitate decreased with a half-life of 3.5 h (Fig. 1*A*). Similar rates of [$^3$H]palmitate turnover was obtained with either a 4-h or shorter 1-h labeling period (data for 1 h not shown). Therefore, the protein and palmitate groups exhibited comparable half-lives, suggesting that PI4KIIα is stably palmitoylated.

*Identification of Candidate PI4KIIα PATs*—We screened all 23 HA-DHHC PATs against Myc-PI4KIIα individually. The extent of HA-DHHC overexpression is shown in supplemental Fig. 1. Among these, DHHC2, DHHC3, DHHC7, DHHC14, DHHC15, and DHHC21 consistently increased [$^3$H]palmitate incorporation into PI4KIIα (Fig. 1*B*, fluorography and Western blot). DHHC3 and DHHC7 were particularly effective, increasing [$^3$H]palmitate incorporation by >3-fold in multiple experiments (Fig. 1*B*, bar graph). Immunofluorescence labeling showed that EGFP-PI4KIIα and endogenous DHHC3 or DHHC7 were both enriched in the TGN and in extra-Golgi vesicles (Fig. 1*C*). The extent of colocalization was evaluated in cells coexpressing EGFP-PI4KIIα and HA-tagged candidate PATs, and we found that either DHHC3 or DHHC7 was at least 80% colocalized with EGFP-PI4KIIα (Fig. 1*D*). Thus, DHHC3 and DHHC7 are prime candidate PI4KIIα PATs.

Multiple approaches were used to establish the role of DHHC3 and DHHC7 in PI4KIIα palmitoylation. First, dominant-negative (DN) DHHC3 and DHHC7 that were mutated from DHHC to DHHS (18) decreased ambient PI4KIIα palmitoylation by 40 and 60%, respectively (Fig. 2*A*). Second, RNAi silencing of DHHC3 or DHHC7 expression decreased PI4KIIα palmitoylation by 80 and 60%, respectively (Fig. 2*B*). The decrease in palmitoylation was confirmed functionally by biochemical extraction (Fig. 2*C*). After RNAi, there was an increase in the ratio of carbonate-extracted (fraction 2) to detergent-extracted (fraction 3) "integral" PI4KIIα from 0.14 to 0.72 or 0.49 for DHHC3 or DHHC7 RNAi, respectively.

Two independent sets of siRNA generated similar results. Depletion of DHHC3 was confirmed by Western blotting (Fig. 2*B*) and immunofluorescence labeling (Fig. 3*A*). Depletion of DHHC7 was established by the decrease in immunofluorescence labeling only (Fig. 3*A*) because the commercially available anti-DHHC7 antibody did not generate a clear signal in Western blotting.

We also examined the effects of DHHC3 or DHHC7 RNAi on PI4KIIα intracellular distribution. Depletion of DHHC3 or DHHC7 by RNAi dispersed PI4KIIα throughout the cytoplasm in small punctae (Fig. 3*A*). Because we have shown previously that palmitoylation promotes PI4KIIα association with the TGN (14), these results supported the conclusion that DHHC3 and DHHC7 palmitoylate PI4KIIα to promote their Golgi targeting.

Unexpectedly, the DHHC3 RNAi cells and, to a lesser extent, the DHHC7 RNAi cells had almost complete loss of perinuclear TGN46 staining (Fig. 3, *A* and *B*). The extent of TGN46 dispersal in the DHHC3 RNAi cells was more pronounced than that observed with PI4KIIα RNAi *per se* (Fig. 3*B*). By comparison, staining of the *cis*-Golgi matrix protein GM130 was much less severely affected than TGN46 in DHHC3-depleted cells (Fig.

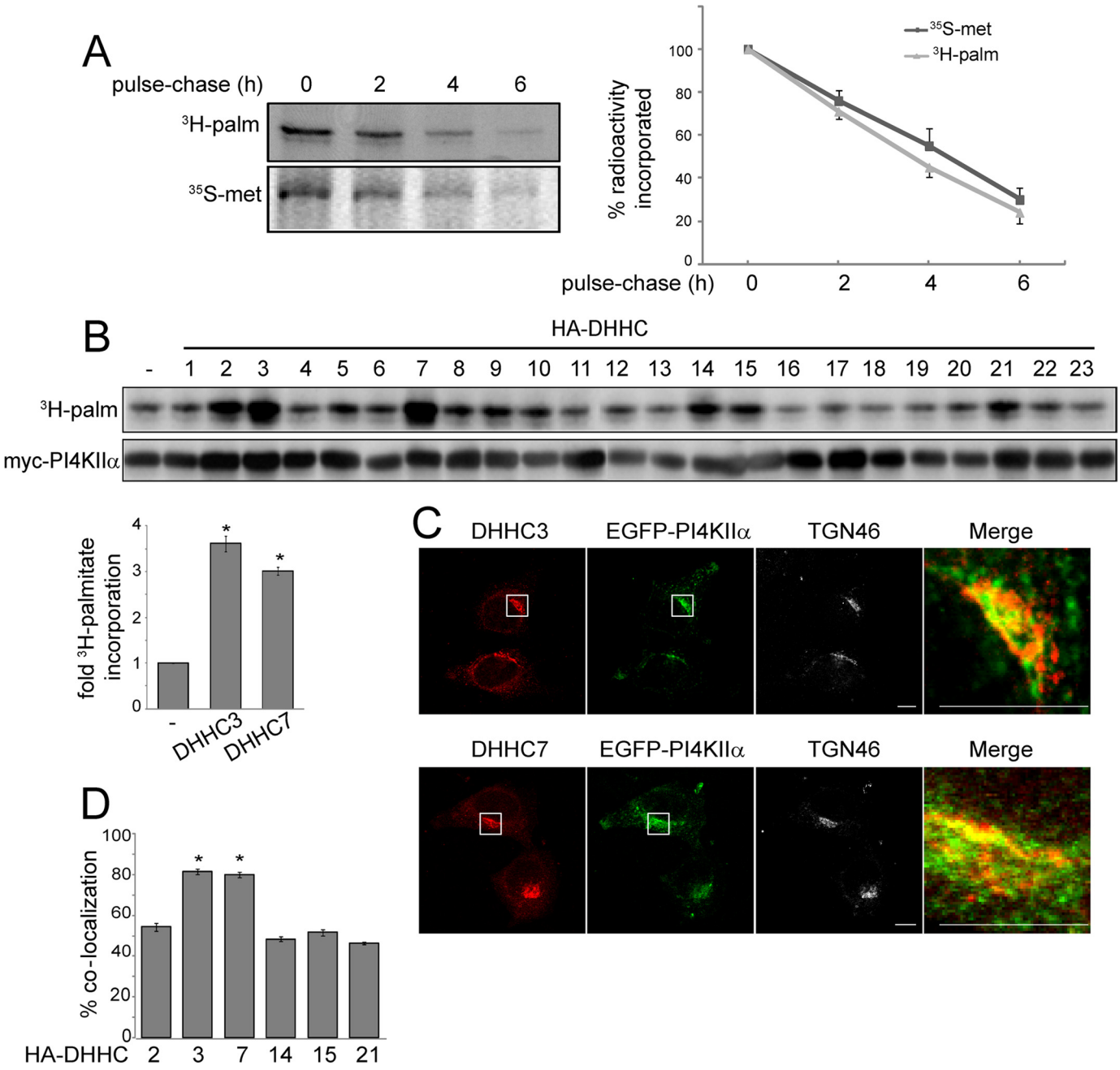


FIGURE 1. **PI4KIIα palmitoylation turnover and PAT screen.** *A*, PI4KIIα protein and palmitate turnover. HEK293 cells were transfected with Myc-PI4KIIα. After metabolic labeling with [$^{35}$S]Met/Cys for 1 h or [$^{3}$H]palmitate (*$^{3}$H-palm*) for 4 h, proteins were chased with unlabeled Met/Cys or palmitate for 2, 4, and 6 h. Cells were lysed and immunoprecipitated with anti-Myc antibody. The immunoprecipitated samples were then separated by SDS-PAGE and analyzed by fluorography. The fluorography intensities were quantified by ImageQuant 5.2 software and are expressed as radioactivity incorporation relative to the control at time 0. Values are means ± S.E. ($n = 3$). *B*, screening for potential PI4KIIα PATs. Individual HA-DHHC PAT cDNA clones were cotransfected with Myc-PI4KIIα into HEK293 cells. Cells were labeled with [$^{3}$H]palmitate, and lysates were analyzed by SDS-PAGE, followed by fluorography. Lysates were subjected to immunoblotting with anti-Myc and anti-HA antibodies (shown in supplemental Fig. 1). The bar graph shows -fold increase in [$^{3}$H]palmitate incorporation (adjusted for Myc-PI4KIIα protein levels) by coexpressed HA-DHHC3 or DHHC7 relative to the control value without expressed DHHC. Values are means ± S.E. ($n = 3$). *, $p < 0.01$. *C*, colocalization of endogenous DHHCs with EGFP-PI4KIIα. HeLa cells were transfected with EGFP-PI4KIIα and then labeled with anti-TGN46 and anti-DHHC3 or anti-DHHC7 antibodies to detect endogenous proteins. The *boxed* areas are enlarged in the merged images to compare the distribution of endogenous DHHC and EGFP-PI4KIIα. *Scale bars* = 10 μm. *D*, percentage colocalization of EGFP-PI4KIIα and HA-DHHC in HeLa cells. Z-stack confocal images were analyzed using the Zeiss LSM 510 ZEN software. Ten randomly chosen cells from each group were analyzed. Values are means ± S.E. *, $p < 0.01$.

3*B*). Thus, these DHHCs are critically important for maintaining the integrity of the TGN. We propose that this is mediated partly by interference with PI4KIIα palmitoylation and hence PI4P generation.

To rule out off-target effects due to RNAi, we also examined the effect of expressing DN-DHHCs on the TGN morphology. In control transfected cells, ~65% of the cells had normal compact TGN46 staining (Fig. 3*C*). In contrast, only 27 and 37% of cells transfected with DN-DHHC3 or DN-DHHC7, respectively, displayed compact TGN staining (Fig. 3*C*). Taken together, our results established that DHHC3 and DHHC7 are individually necessary for TGN integrity and functions, includ-

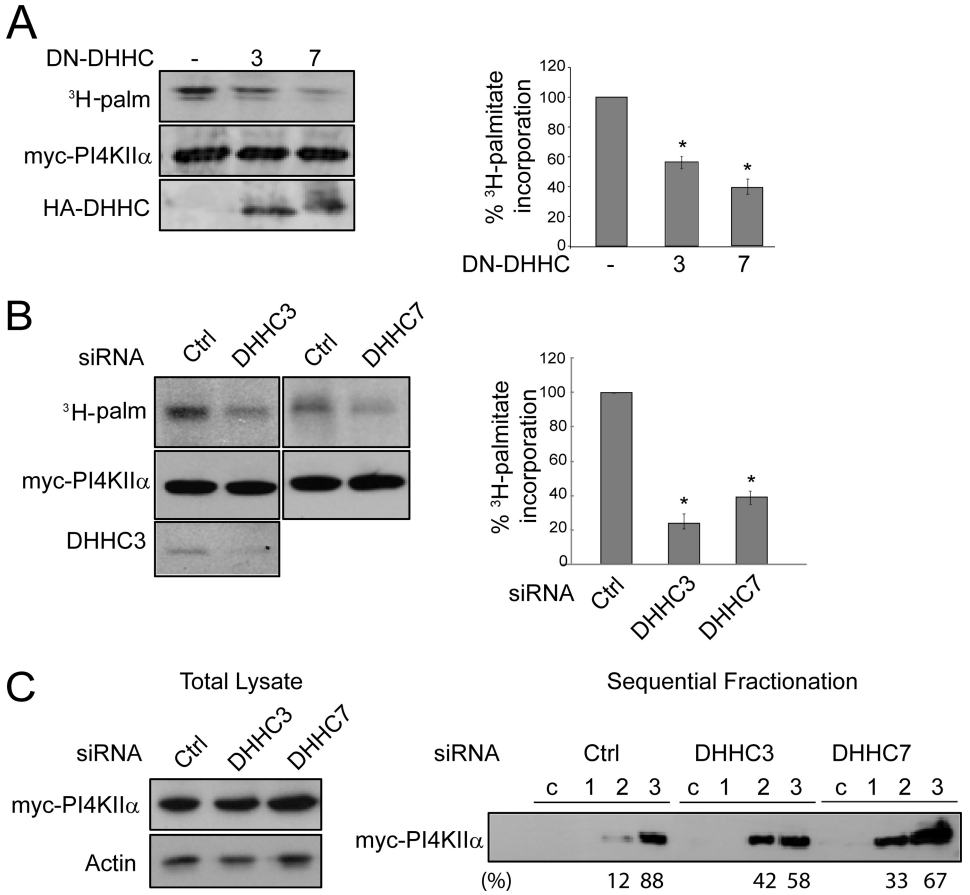


FIGURE 2. **Effect of DN-DHHC3 or DN-DHHC7 inhibition or silencing on PI4KIIα palmitoylation.** Representative Western blots and fluorography are shown. Palmitoylation was quantified by ImageQuant 5.2 software and is expressed as a percentage of the control. Values are means ± S.E. ($n = 3$). *, $p < 0.01$. *A*, overexpression of DN-DHHC3 or DN-DHHC7. COS-7 cells were cotransfected with Myc-PI4KIIα and either DN-DHHC3 or DN-DHHC7 and labeled with [$^3$H]palmitate (*$^3$H-palm*). Myc-PI4KIIα was immunoprecipitated, resolved by SDS-PAGE, and analyzed by fluorography and Western blotting. *Left*, Western blot and fluorography of a representative experiment; *right*, percentage $^3$H palmitoylation. *B*, DHHC3 or DHHC7 RNAi. HeLa cells were transfected with DHHC or control (*Ctrl*) siRNA for 48 h, followed by Myc-PI4KIIα transfection for another 16 h, and then labeled with [$^3$H]palmitate for 4 h. Endogenous DHHC3 was detected with anti-DHHC3 antibody in Western blots. *C*, DHHC RNAi effect on PI4KIIα membrane extractability. Cells were homogenized, and the post-nuclear supernatant (lysate) was analyzed by Western blotting (*left*). The lysate was centrifuged at 200,000 × *g* to obtain the cytosolic fraction (*c*) and membrane pellet. Membranes were extracted sequentially with 1 M NaCl, 0.1 M $Na_2CO_3$, and 1% Triton-X100 (fractions 1–3, respectively) (*right*). Equivalent amounts of each fraction were analyzed by immunoblotting with anti-Myc antibody. The percentage of total PI4KIIα in each fraction is indicated below the Western blot.

ing PI4KIIα Golgi recruitment and palmitoylation. Additional studies will be required to identify other mechanisms whereby DHHCs contribute to TGN integrity.

*Association of PI4KIIα with DHHC3 and DHHC7*—Previous coexpression studies have shown that interactions of DHHCs with some of their substrate proteins are sufficiently stable to be detected biochemically (17, 19, 31–33). Using pulldown assays, we found that both WT and palmitoylation-defective (DN) HA-tagged DHHC3 and DHHC7 associated with immunoprecipitated Myc-PI4KIIα (Fig. 4*A*, *left*) and, reciprocally, Myc-PI4KIIα with immunoprecipitated HA-DHHC3 (Fig. 4*B*, *left*). The interaction was specific because Myc-PI4KIIα did not co-immunoprecipitate with non-candidate HA-DHHC18 or HA-DHHC23 (Fig. 4*A*, *right*).

We examined the requirements for this interaction by using PI4KIIα mutants. The truncation mutant containing the catalytic domain (amino acids 93–478) (Fig. 4*B*, *Cat*) and the embedded CCPCC palmitoylation motif associated with DHHC3, but the non-palmitoylatable SSPSS mutant did not. Thus, PI4KIIα interacts with DHHC3 and DHHC7, and its CCPCC palmitoylation motif, but not the N- or C-terminal extensions, is required for interaction.

*Dependence of PI4KIIα Palmitoylation on Cholesterol*—Although previous studies have shown independently that PI4KIIα catalytic activity and Golgi localization are dependent on palmitoylation (14) as well as on cholesterol (9, 16, 34), the relation between palmitoylation and cholesterol has not been examined. To examine this relation, we manipulated cholesterol in intact cells using the MβCD depletion and repletion protocols that have previously been optimized to examine effects on PI4KIIα behavior in cells and in membranes (9, 16). MβCD decreased Myc-PI4KIIα co-immunoprecipitation with HA-DHHC7 (Fig. 4*C*). Conversely, association was restored by reintroduction of cholesterol complexed with MβCD. Similar results were obtained with HA-DHHC3 (data not shown). Furthermore, cholesterol depletion/repletion also reversibly impacted PI4KIIα palmitoylation (Fig. 5*A*).

Previous independent studies have shown in discontinuous gradient centrifugation experiments that PI4KIIα (14) and DHHC3 and DHHC7 (17) were partially associated with deter-

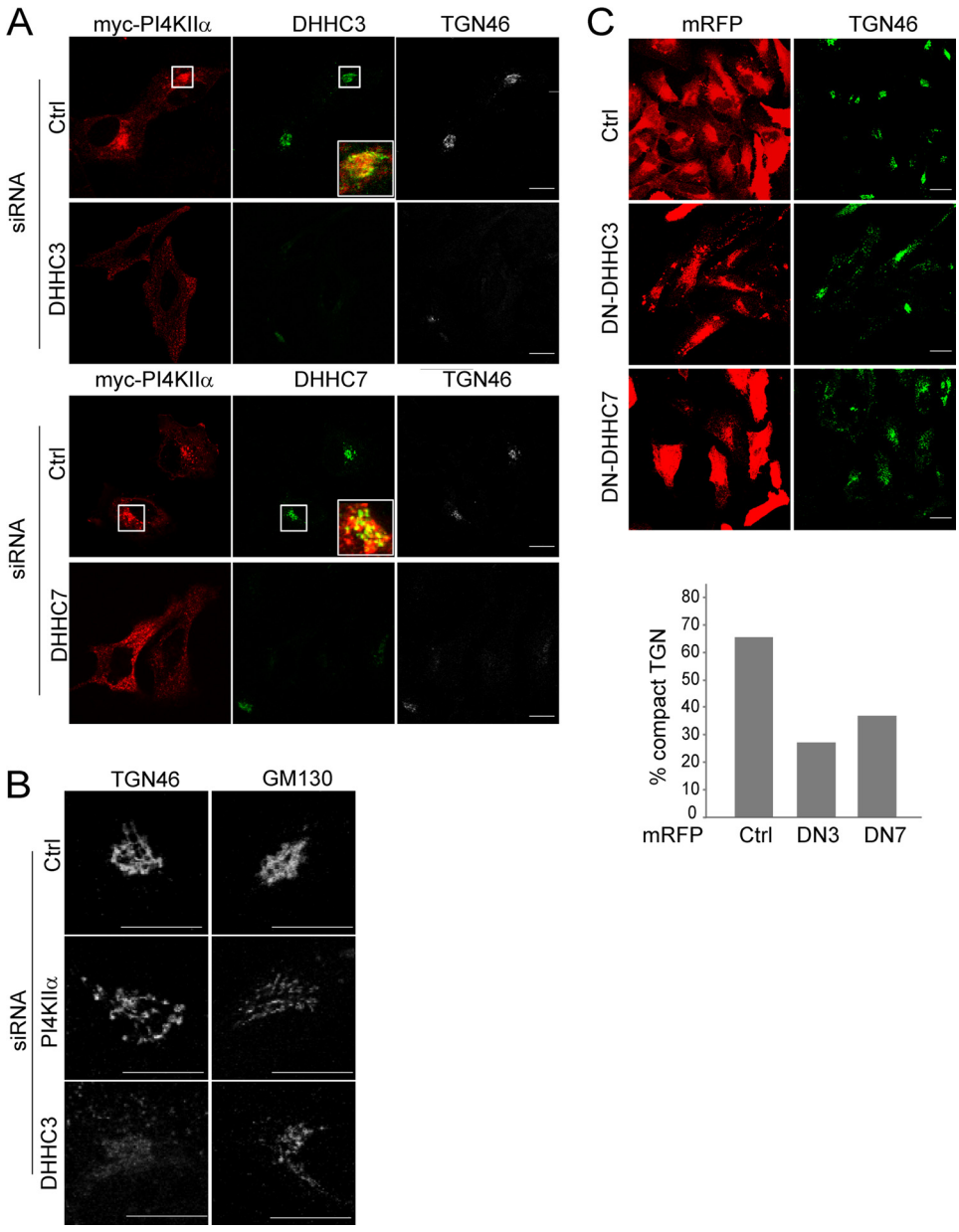


FIGURE 3. **Effects of DHHC3 or DHHC7 inhibition or silencing on PI4KIIα localization and TGN integrity.** *A*, DHHC RNAi effects on PI4KIIα localization. HeLa cells transfected with DHHC siRNA for 68 h and Myc-PI4KIIα for the last 20 h were labeled with anti-Myc, anti-DHHC3 or anti-DHHC7, and anti-TGN46 antibodies. *Scale bars* = 10 μm. *Boxed* areas were enlarged to show merged images of Myc-PI4KIIα and DHHCs. *B*, effects of PI4KIIα or DHHC3 RNAi on the TGN and *cis*-Golgi. Cells transfected with siRNA against DHHC or PI4KIIα for 48 h were labeled with either anti-TGN46 (a TGN marker) or anti-GM130 (a *cis*-Golgi marker) antibody. *Scale bars* = 10 μm. *C*, effect of overexpression of monomer red fluorescent protein (*mRFP*)-tagged DN-DHHC3 or DN-DHHC7 on TGN integrity. Cells were stained with anti-TGN46 antibody. Cells were scored visually in a blinded fashion for compact (normal) *versus* expanded (abnormal) TGN46 staining. 100 cells were scored per condition. *Scale bars* = 10 μm. The percentage of monomer red fluorescent protein-positive cells with compact TGN46 staining is displayed in the bar graph. *Ctrl*, control.

gent-insoluble light membrane fractions (rafts). We confirmed that this is indeed the case in parallel experiments (Fig. 5*B*). We compared the effects of cholesterol depletion on the extractability of PI4KIIα and DHHCs. MβCD decreased the "integral" membrane association of PI4KIIα, but not DHHC3 or DHHC7 (Fig. 5*B*). These results clearly established that PI4KIIα is a peripheral membrane protein that becomes "integrally" associated after cholesterol-dependent palmitoylation, whereas DHHC3 and DHHC7 are *bona fide* transmembrane proteins (35) that are not dependent on cholesterol for membrane insertion.

Cholesterol depletion decreased PI4KIIα association with the perinuclear Golgi region and increased PI4KIIα in cytoplasmic vesicles (Fig. 5*C*), in agreement with a previous report (9). In contrast, cholesterol depletion did not induce dispersal of DHHC3 and DHHC7 from the Golgi and also did not disrupt perinuclear TGN46 staining to a similar extent, at least at the resolution of the immunofluorescence microscopy (Fig. 5*C*). These differences suggested that cholesterol depletion induces dispersal of PI4KIIα from the Golgi by decreasing palmitoylation and not directly as a result of disruption of DHHC localization in the Golgi or disruption of the TGN *per se*.

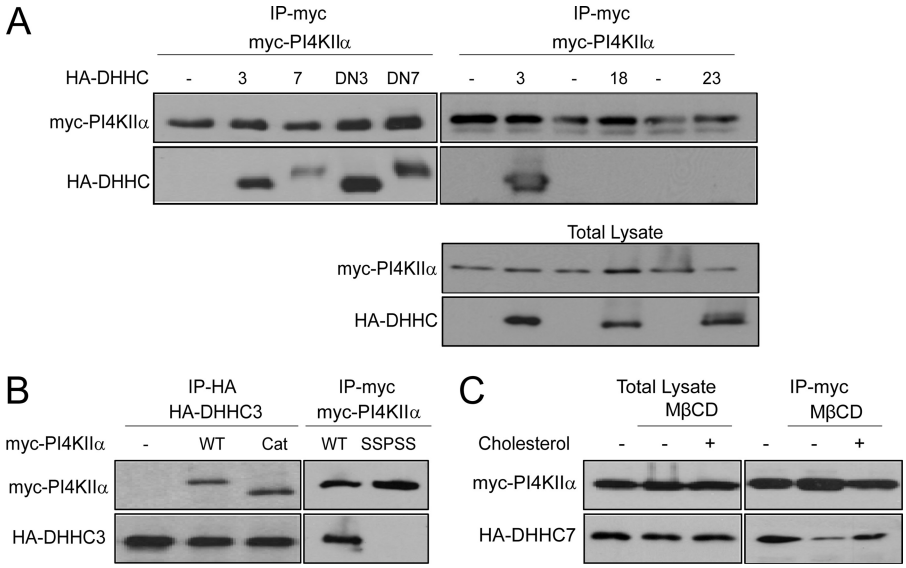


FIGURE 4. **PI4KIIα association with DHHC3 or DHHC7.** COS-7 cells were cotransfected with Myc-PI4KIIα and HA-DHHC. *A*, pulldown assays. *Upper*, Myc-PI4KIIα was immunoprecipitated (*IP*) using anti-Myc antibody, and the presence of HA-tagged WT or DN-DHHCs was detected by immunoblotting with anti-HA antibody. *Lower*, expression level of Myc-4KIIα and HA-DHHCs in total lysate detected by Western blotting. *B*, *left*, anti-HA antibody was used to immunoprecipitate HA-DHHC3, and associated full-length Myc-PI4KIIα or the Myc-PI4KIIα catalytic (*Cat*) domain (amino acids 93–478) was detected using anti-Myc antibody; *right*, the non-palmitoylatable PI4KIIα SSPSS mutant did not co-immunoprecipitate with HA-DHHC3. *C*, cholesterol dependence. HeLa cells overexpressing Myc-PI4KIIα and HA-DHHC7 were treated with or without 10 mM MβCD in DMEM for 30 min, washed twice, and incubated in DMEM with 5% lipoprotein-deficient serum with or without 2.5 mM water-soluble cholesterol (complexed with MβCD) for 2 h. Myc-PI4KIIα was immunoprecipitated, and associated HA-DHHC7 was detected using anti-HA antibody.

The impact of cholesterol depletion on PI4P levels in the Golgi was examined by immunofluorescence microscopy using anti-PI4P antibody. This approach was made possible by the availability of a recently optimized fixation/permeabilization protocol that was optimized to preserve Golgi/endomembrane PI4P (26). Cholesterol depletion reduced Golgi PI4P levels by 70%, and Golgi PI4P was restored by cholesterol repletion (Fig. 5*D*). Taken together, our results established that cholesterol is critical for recruitment of PI4KIIα to the Golgi by promoting its association with Golgi-localized DHHC3 and DHHC7. Subsequently, palmitoylation and activation of PI4KIIα increase PI4P generation at the Golgi.

## DISCUSSION

*S*-Palmitoylation regulates the subcellular localization, activity, and raft association of multiple proteins (21–23, 36, 37). Although many proteins are dynamically palmitoylated, others, such as caveolin (29), are stably palmitoylated. Here, we have demonstrated, using pulse-chase experiments, that the palmitoyl groups of PI4KIIα remain attached to the protein almost throughout its entire life time, indicating that PI4KIIα is stably palmitoylated. We identified the DHHC PATs that palmitoylate PI4KIIα and showed that palmitoylation provides a structural signal for PI4KIIα Golgi targeting, integral membrane anchoring, and catalytic activation and, importantly, that palmitoylation is cholesterol-dependent.

Previous studies have shown that the majority of DHHCs are found in the Golgi or endoplasmic reticulum, but a minority are also present at extra-Golgi sites and on the plasma membrane (38–41). Here, we have shown that PI4KIIα can be palmitoylated by at least six DHHC PATs (DHHC2, DHHC3, DHHC7, DHHC14, DHHC15, and DHHC21). The profile of positive PATs is similar, but not identical, to that reported for several other unrelated proteins. For example, although endothelial NOS and stathmin are palmitoylated by DHHC2, DHHC3, and DHHC7 (17, 39), endothelial NOS is not palmitoylated by DHHC14 or DHHC15, and stathmin is not palmitoylated by DHHC14 or DHHC21. DHHC2 is found on the plasma membrane and in vesicles that have the characteristics of recycling endosomes (40, 41). Because PI4KIIα is enriched in the Golgi and also in endosomes (7, 8, 10), the possibility that it may be palmitoylated by DHHC2 at extra-Golgi sites should be explored.

In light of our primary interest in PI4KIIα palmitoylation in the Golgi, we focused on DHHC3 and DHHC7 in this study. We have shown, using DN-PATs and PAT knockdown by RNAi, that DHHC3 and DHHC7 are *bona fide* PI4KIIα PATs that are colocalized and associated with PI4KIIα. Binding is independent of the ability of PATs to palmitoylate because both the WT and palmitoylation-defective DN-DHHCs bind PI4KIIα. However, because the PI4KIIα SSPSS mutant does not bind to DHHCs, it appears that the CCPCC palmitoylation motif is nevertheless required. Importantly, non-candidate DHHC18 and DHHC23 did not associate with PI4KIIα. These features suggest that PI4KIIα binds candidate DHHCs specifically in a manner that is dependent on the CCPCC motif, and it becomes palmitoylated by the catalytically active DHHC after physical association. Additional studies will be required to determine whether PI4KIIα binds DHHC3 or DHHC7 directly or indirectly.

Our results provide a mechanistic model to explain how PI4KIIα is preferentially targeted to the Golgi for palmitoylation. We have previously proposed a multistep process (14): 1) although non-palmitoylated PI4KIIα has high intrinsic membrane-binding ability and can potentially bind to all mem-

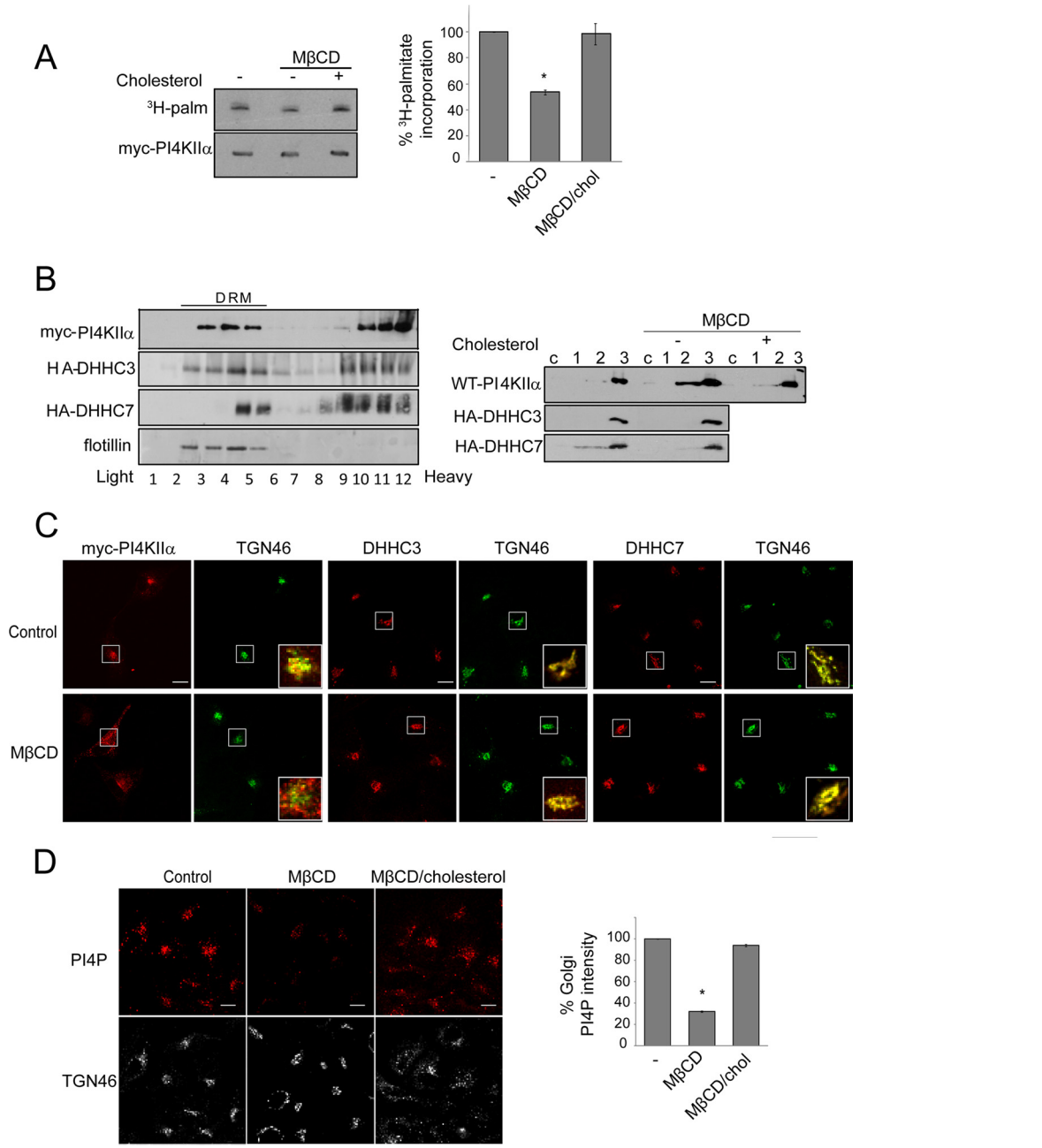


FIGURE 5. **Effects of cholesterol depletion/repletion.** *A*, PI4KIIα palmitoylation. COS-7 cells overexpressing Myc-PI4KIIα were subjected to cholesterol depletion and repletion and labeled with [$^3$H]palmitate (*$^3$H-palm*). Myc-PI4KIIα was immunoprecipitated, resolved by SDS-PAGE, and analyzed by fluorography and immunoblotting. *Left*, fluorography and immunoblotting; *right*, percentage $^3$H palmitoylation, normalized against the amount of Myc-PI4KIIα. Values are means ± S.E. ($n = 3$). *, $p < 0.01$. *B*, raft association and "integral" membrane association. COS-7 cells were transfected with Myc-PI4KIIα, HA-DHHC3, or HA-DHHC7. *Left*, association with low buoyant density (light) detergent-resistant membranes (*DRM*). Cells were homogenized in 1% Brij 98 and subjected to centrifugation in a discontinuous sucrose step gradient. Protein distribution in the collected fractions was monitored by immunoblotting with anti-Myc (PI4KIIα), anti-HA (DHHC), and anti-flotillin (a detergent-resistant membrane marker) antibodies. *Right*, "integral" membrane association. Cell lysates were centrifuged, and the 200,000 × *g* supernatant (*c*) was collected. The pellets were extracted sequentially with NaCl, $Na_2CO_3$, and 1% Triton X-100 (fractions 1–3, respectively) and subjected to Western blotting. *C*, Golgi localization. Cells were labeled with anti-Myc (PI4KIIα), anti-DHHC3 or anti-DHHC7, and anti-TGN46 antibodies. *Scale bars* = 10 μm. The *insets* show the enlarged merged images of green and red channels. *D*, Golgi PI4P. Cells were fixed and permeabilized using a protocol optimized for the detection of Golgi PI4P with anti-PI4P antibody. PI4P intensity in the Golgi region (marked by TGN46 staining) was quantified using ImageJ software, averaged by cell numbers, and is expressed relative to the control value. *Scale bars* = 10 μm. Values are means ± S.E. ($n = 25$). *, $p < 0.01$. *chol*, cholesterol.

branes, newly synthesized (not yet palmitoylated) PI4KIIα is nevertheless preferentially recruited to the Golgi by binding to a hypothetical Golgi "docking protein"; 2) PI4KIIα penetrates the Golgi membrane bilayer by virtue of its amphipathic membrane-anchoring loop; and 3) this positions the CCPCC motif against the membrane and brings it within reach of the Golgi-localized DHHCs. These cysteines are palmitoylated, and the covalently attached palmitate groups provide a strong secondary anchor to kinetically trap PI4KIIα in the Golgi and in Golgi-derived membranes (14).

The data presented here suggest that the DHHCs are the docking proteins and also the PATs for PI4KIIα. The multistep

model can therefore be streamlined considerably. This streamlined model for PI4KIIα Golgi recruitment and palmitoylation provides new insight into how cholesterol regulates PI4KIIα. Because PI4KIIα and DHHCs are partially raft-associated and cholesterol promotes PI4KIIα association with DHHC3 and DHHC7, co-partitioning of PI4KIIα and DHHCs in raft microdomains should promote their interaction and result in higher levels of PI4KIIα palmitoylation. This model can explain the previous observation that PI4KIIα in isolated raft membranes is catalytically more active than that in non-raft membranes (9, 16, 34). Cholesterol depletion has a minimal effect on DHHC association with the Golgi *per se*, but it decreases PI4KIIα association with DHHCs presumably by dispersing raft microdomains to decrease encounters between PI4KIIα and DHHCs. We also showed for the first time in cells that cholesterol depletion dramatically decreases Golgi PI4P, consistent with a decrease in the interaction of PI4KIIα with DHHCs and, consequently, its palmitoylation.

In this study, we also reviewed for the first time new information about the role of DHHC3 and DHHC7 in maintaining Golgi integrity. Depletion of either DHHC3 or DHHC7 by RNAi or expression of DN constructs disrupts the TGN to a greater extent than PI4KIIα RNAi *per se*. These results strongly suggest that DHHCs regulate Golgi integrity partly, *but not entirely*, by PI4KIIα palmitoylation and PI4P generation to maintain the organelle identity of the Golgi. Because DHHC3 and DHHC7 palmitoylate multiple proteins at the Golgi (33, 41, 42), it is not possible at present to definitively assign a cause and effect relation for any one affected Golgi protein. Our discovery of the unanticipated role of DHHCs in maintaining TGN integrity expands our understanding of DHHC biology.

## REFERENCES


1. Graham, T. R., and Burd, C. G. (2011) Coordination of Golgi functions by phosphatidylinositol 4-kinases. *Trends Cell Biol.* **21,** 113–121
2. Santiago-Tirado, F. H., Legesse-Miller, A., Schott, D., and Bretscher, A. (2011) PI4P and Rab inputs collaborate in myosin V-dependent transport of secretory compartments in yeast. *Dev. Cell* **20,** 47–59
3. Balla, A., Kim, Y. J., Varnai, P., Szentpetery, Z., Knight, Z., Shokat, K. M., and Balla, T. (2008) Maintenance of hormone-sensitive phosphoinositide pools in the plasma membrane requires phosphatidylinositol 4-kinase IIIα. *Mol. Biol. Cell* **19,** 711–721
4. Balla, A., and Balla, T. (2006) Phosphatidylinositol 4-kinases: old enzymes with emerging functions. *Trends Cell Biol.* **16,** 351–361
5. Wang, Y. J., Wang, J., Sun, H. Q., Martinez, M., Sun, Y. X., Macia, E., Kirchhausen, T., Albanesi, J. P., Roth, M. G., and Yin, H. L. (2003) Phosphatidylinositol 4-phosphate regulates targeting of clathrin adaptor AP-1 complexes to the Golgi. *Cell* **114,** 299–310
6. Weixel, K. M., Blumental-Perry, A., Watkins, S. C., Aridor, M., and Weisz, O. A. (2005) Distinct Golgi populations of phosphatidylinositol 4-phosphate regulated by phosphatidylinositol 4-kinases. *J. Biol. Chem.* **280,** 10501–10508
7. Balla, A., Tuymetova, G., Barshishat, M., Geiszt, M., and Balla, T. (2002) Characterization of type II phosphatidylinositol 4-kinase isoforms reveals association of the enzymes with endosomal vesicular compartments. *J. Biol. Chem.* **277,** 20041–20050
8. Wei, Y. J., Sun, H. Q., Yamamoto, M., Wlodarski, P., Kunii, K., Martinez, M., Barylko, B., Albanesi, J. P., and Yin, H. L. (2002) Type II phosphatidylinositol 4-kinase β is a cytosolic and peripheral membrane protein that is recruited to the plasma membrane and activated by Rac-GTP. *J. Biol. Chem.* **277,** 46586–46593
9. Minogue, S., Chu, K. M., Westover, E. J., Covey, D. F., Hsuan, J. J., and Waugh, M. G. (2010) Relationship between phosphatidylinositol 4-phosphate synthesis, membrane organization, and lateral diffusion of PI4KIIα at the *trans*-Golgi network. *J. Lipid Res.* **51,** 2314–2324
10. Minogue, S., Waugh, M. G., De Matteis, M. A., Stephens, D. J., Berditchevski, F., and Hsuan, J. J. (2006) Phosphatidylinositol 4-kinase is required for endosomal trafficking and degradation of the EGF receptor. *J. Cell Sci.* **119,** 571–581
11. Wang, J., Sun, H. Q., Macia, E., Kirchhausen, T., Watson, H., Bonifacino, J. S., and Yin, H. L. (2007) PI4P promotes the recruitment of the GGA adaptor proteins to the *trans*-Golgi network and regulates their recognition of the ubiquitin sorting signal. *Mol. Biol. Cell* **18,** 2646–2655
12. Pizarro-Cerdá, J., Payrastre, B., Wang, Y. J., Veiga, E., Yin, H. L., and Cossart, P. (2007) Type II phosphatidylinositol 4-kinases promote *Listeria monocytogenes* entry into target cells. *Cell. Microbiol.* **9,** 2381–2390
13. Salazar, G., Craige, B., Wainer, B. H., Guo, J., De Camilli, P., and Faundez, V. (2005) Phosphatidylinositol-4-kinase type IIα is a component of adaptor protein-3-derived vesicles. *Mol. Biol. Cell* **16,** 3692–3704
14. Barylko, B., Mao, Y. S., Wlodarski, P., Jung, G., Binns, D. D., Sun, H. Q., Yin, H. L., and Albanesi, J. P. (2009) Palmitoylation controls the catalytic activity and subcellular distribution of phosphatidylinositol 4-kinase IIα. *J. Biol. Chem.* **284,** 9994–10003
15. Barylko, B., Gerber, S. H., Binns, D. D., Grichine, N., Khvotchev, M., Südhof, T. C., and Albanesi, J. P. (2001) A novel family of phosphatidylinositol 4-kinases conserved from yeast to humans. *J. Biol. Chem.* **276,** 7705–7708
16. Waugh, M. G., Minogue, S., Chotai, D., Berditchevski, F., and Hsuan, J. J. (2006) Lipid and peptide control of phosphatidylinositol 4-kinase IIα activity on Golgi-endosomal rafts. *J. Biol. Chem.* **281,** 3757–3763
17. Fernández-Hernando, C., Fukata, M., Bernatchez, P. N., Fukata, Y., Lin, M. I., Bredt, D. S., and Sessa, W. C. (2006) Identification of Golgi-localized acyltransferases that palmitoylate and regulate endothelial nitric-oxide synthase. *J. Cell Biol.* **174,** 369–377
18. Fukata, Y., Iwanaga, T., and Fukata, M. (2006) Systematic screening for palmitoyltransferase activity of the DHHC protein family in mammalian cells. *Methods* **40,** 177–182
19. Fukata, M., Fukata, Y., Adesnik, H., Nicoll, R. A., and Bredt, D. S. (2004) Identification of PSD-95 palmitoylating enzymes. *Neuron* **44,** 987–996
20. Yanai, A., Huang, K., Kang, R., Singaraja, R. R., Arstikaitis, P., Gan, L., Orban, P. C., Mullard, A., Cowan, C. M., Raymond, L. A., Drisdel, R. C., Green, W. N., Ravikumar, B., Rubinsztein, D. C., El-Husseini, A., and Hayden, M. R. (2006) Palmitoylation of huntingtin by HIP14 is essential for its trafficking and function. *Nat. Neurosci.* **9,** 824–831
21. Greaves, J., and Chamberlain, L. H. (2011) DHHC palmitoyltransferases: substrate interactions and (patho)physiology. *Trends Biochem. Sci.* **36,** 245–253
22. Nadolski, M. J., and Linder, M. E. (2007) Protein lipidation. *FEBS J.* **274,** 5202–5210
23. Fukata, Y., and Fukata, M. (2010) Protein palmitoylation in neuronal development and synaptic plasticity. *Nat. Rev. Neurosci.* **11,** 161–175
24. Claas, C., Stipp, C. S., and Hemler, M. E. (2001) Evaluation of prototype transmembrane 4 superfamily protein complexes and their relation to lipid rafts. *J. Biol. Chem.* **276,** 7974–7984
25. El-Din El-Husseini, A., Schnell, E., Dakoji, S., Sweeney, N., Zhou, Q., Prange, O., Gauthier-Campbell, C., Aguilera-Moreno, A., Nicoll, R. A., and Bredt, D. S. (2002) Synaptic strength regulated by palmitate cycling on PSD-95. *Cell* **108,** 849–863
26. Hammond, G. R., Schiavo, G., and Irvine, R. F. (2009) Immunocytochemical techniques reveal multiple, distinct cellular pools of PtdIns4P and PtdIns(4,5)$P_2$. *Biochem. J.* **422,** 23–35
27. Jia, L., Linder, M. E., and Blumer, K. J. (2011) $G_{i/o}$ signaling and the palmitoyltransferase DHHC2 regulate palmitate cycling and shuttling of RGS7 family-binding protein. *J. Biol. Chem.* **286,** 13695–13703
28. Greaves, J., and Chamberlain, L. H. (2011) Differential palmitoylation regulates intracellular patterning of SNAP25. *J. Cell Sci.* **124,** 1351–1360
29. Parat, M. O., and Fox, P. L. (2001) Palmitoylation of caveolin-1 in endothelial cells is post-translational but irreversible. *J. Biol. Chem.* **276,** 15776–15782
30. Martin, B. R., Wang, C., Adibekian, A., Tully, S. E., and Cravatt, B. F. (2012)

Global profiling of dynamic protein palmitoylation. *Nat. Methods* **9,** 84–89
31. Greaves, J., Salaun, C., Fukata, Y., Fukata, M., and Chamberlain, L. H. (2008) Palmitoylation and membrane interactions of the neuroprotective chaperone cysteine string protein. *J. Biol. Chem.* **283,** 25014–25026
32. Greaves, J., Gorleku, O. A., Salaun, C., and Chamberlain, L. H. (2010) Palmitoylation of the SNAP25 protein family: specificity and regulation by DHHC palmitoyltransferases. *J. Biol. Chem.* **285,** 24629–24638
33. Tsutsumi, R., Fukata, Y., Noritake, J., Iwanaga, T., Perez, F., and Fukata, M. (2009) Identification of G protein α subunit-palmitoylating enzyme. *Mol. Cell. Biol.* **29,** 435–447
34. Waugh, M. G., Chu, K. M., Clayton, E. L., Minogue, S., and Hsuan, J. J. (2011) Detergent-free isolation and characterization of cholesterol-rich membrane domains from *trans*-Golgi network vesicles. *J. Lipid Res.* **52,** 582–589
35. Mitchell, D. A., Vasudevan, A., Linder, M. E., and Deschenes, R. J. (2006) Protein palmitoylation by a family of DHHC protein *S*-acyltransferases. *J. Lipid Res.* **47,** 1118–1127
36. Linder, M. E., and Deschenes, R. J. (2007) Palmitoylation: policing protein stability and traffic. *Nat. Rev. Mol. Cell Biol.* **8,** 74–84
37. Greaves, J., and Chamberlain, L. H. (2007) Palmitoylation-dependent protein sorting. *J. Cell Biol.* **176,** 249–254
38. Ohno, Y., Kihara, A., Sano, T., and Igarashi, Y. (2006) Intracellular localization and tissue-specific distribution of human and yeast DHHC cysteine-rich domain-containing proteins. *Biochim. Biophys. Acta* **1761,** 474–483
39. Levy, A. D., Devignot, V., Fukata, Y., Fukata, M., Sobel, A., and Chauvin, S. (2011) Subcellular Golgi localization of stathmin family proteins is promoted by a specific set of DHHC palmitoyltransferases. *Mol. Biol. Cell* **22,** 1930–1942
40. Greaves, J., Carmichael, J. A., and Chamberlain, L. H. (2011) The palmitoyltransferase DHHC2 targets a dynamic membrane cycling pathway: regulation by a C-terminal domain. *Mol. Biol. Cell* **22,** 1887–1895
41. Noritake, J., Fukata, Y., Iwanaga, T., Hosomi, N., Tsutsumi, R., Matsuda, N., Tani, H., Iwanari, H., Mochizuki, Y., Kodama, T., Matsuura, Y., Bredt, D. S., Hamakubo, T., and Fukata, M. (2009) Mobile DHHC palmitoylating enzyme mediates activity-sensitive synaptic targeting of PSD-95. *J. Cell Biol.* **186,** 147–160
42. Huang, K., Sanders, S., Singaraja, R., Orban, P., Cijsouw, T., Arstikaitis, P., Yanai, A., Hayden, M. R., and El-Husseini, A. (2009) Neuronal palmitoyl acyltransferases exhibit distinct substrate specificity. *FASEB J.* **23,** 2605–2615